

# Universal properties of single particle excitations across the many-body localization transition

Atanu Jana<sup>1,3</sup>, V. Ravi Chandra<sup>1,3</sup>, Arti Garg<sup>2,3</sup>

<sup>1</sup> School of Physical Sciences, National Institute of Science Education and Research Bhubaneswar, Jatni, Odisha 752050, India

<sup>2</sup> Theory Division, Saha Institute of Nuclear Physics,  
1/AF Bidhannagar, Kolkata 700 064, India and

<sup>3</sup> Homi Bhabha National Institute, Training School Complex, Anushaktinagar, Mumbai 400094, India

Understanding the nature of the transition from the delocalized to the many-body localized (MBL) phase is an important unresolved issue. To probe the nature of the MBL transition, we investigate the universal properties of single-particle excitations produced in highly excited many-body eigenstates of a disordered interacting quantum many-body system. In a class of one-dimensional spinless fermionic models, we study the finite size scaling of the ratio of typical to average values of the single-particle local density of states and the scattering rates across the MBL transition. Our results indicate that the MBL transition in this class of one-dimensional models of spinless fermions is continuous in nature. The critical exponent  $\nu$  with which the correlation length  $\xi$  diverges at the transition point  $W_c$ ,  $\xi \sim |W - W_c|^{-\nu}$ , satisfies the Chayes-Chayes-Fisher-Spencer (CCFS) bound  $\nu \geq 2/d$  where  $d$  is the physical dimension of the system. The transition point  $W_c$  and the critical exponent  $\nu$  do not change significantly with the range of interactions between fermions as long as the hopping is short range.

The role of disorder in quantum many-body systems has been a major focus of the condensed matter physics research for several decades. Anderson localization is a fascinating example of a disorder-driven phenomenon in which a non-interacting quantum system can become diffusion-less in the presence of strong enough disorder [1]. Almost two decades ago, Anderson localization was generalised for the case of interacting quantum systems [2] which is known as many-body localization (MBL) [3]. In the MBL phase, a subsystem of an isolated quantum system does not thermalize with the rest of the system serving as its bath. This is due to the system's non-ergodicity [3–5] and strong memory of the initial states [6–18]. In the MBL phase even highly excited states of an isolated system obey area law of entanglement entropy rather than the volume law [5, 19–24]. This is also reflected in the slow growth of subsystem entanglement for the MBL phase compared to the delocalized phase [18, 25–27]. Systems in the MBL phase have also been shown to have local integrals of motion [28–30]. Although the MBL phase has been rigorously proved to exist in strongly disordered 1-dimensional spin chains with short range interactions [31], broad agreement about the nature of the transition from the delocalized phase to the MBL phase has been elusive. We provide strong evidence in favor of a continuous transition from the delocalized phase to the MBL phase in this work.

Real-space renormalization group studies predicted a critical point at the transition from the delocalized phase to the MBL phase with the correlation length  $\xi$  having a power-law divergence  $\xi \sim |W - W_c|^{-\nu}$  at the transition point  $W_c$  with the critical exponent  $\nu \sim 3$  [32–36] which satisfies the Chayes-Chayes-Fisher-Spencer (CCFS) bound  $\nu \geq 2/d$  where  $d$  is the physical

dimension of the system [37, 38]. It was established by Harris [39] that if  $\nu \geq 2/d$  for a clean system undergoing a continuous transition then disorder is irrelevant in the renormalisation group sense. A more general argument by CCFS concludes that  $\nu \geq 2/d$  holds true for all systems with quenched random disorder that undergo a continuous transition including the localization transition, irrespective of whether there is an analogous transition in the clean system [37, 38]. In fact, the finite size scaling of the Anderson localization transition for the non-interacting model in higher dimensions ( $d \geq 3$ ) has been shown to satisfy this bound for the critical exponent [40–44]. In the analysis of the MBL transition one issue of concern has been that barring a few exceptions [45], most of the numerical studies which investigated finite size scaling of quantities like entanglement entropy and level spacing ratio found the critical exponent  $\nu \sim 1$  violating the CCFS bound [5, 20, 46, 47]. The violation of CCFS bound, as well as the disparity between phenomenology and numerical calculations prompted a modified renormalization group approach [48–50] that predicted a Kosterlitz-Thouless (KT) like transition. This approach, which is based on avalanche mechanism of delocalization to MBL transition [51, 52], has been explored in some recent numerical studies [53–55]. In short, there is no agreement on the nature of the delocalization to MBL transition, so it is critical to identify appropriate physical observables that can characterize the MBL transition.

With this motivation, in this work we investigate the single-particle excitations obtained via infinite temperature single-particle Green's function in real space across the MBL transition. Green's functions in the Fock space have been studied in the context of MBL [56–58], how-

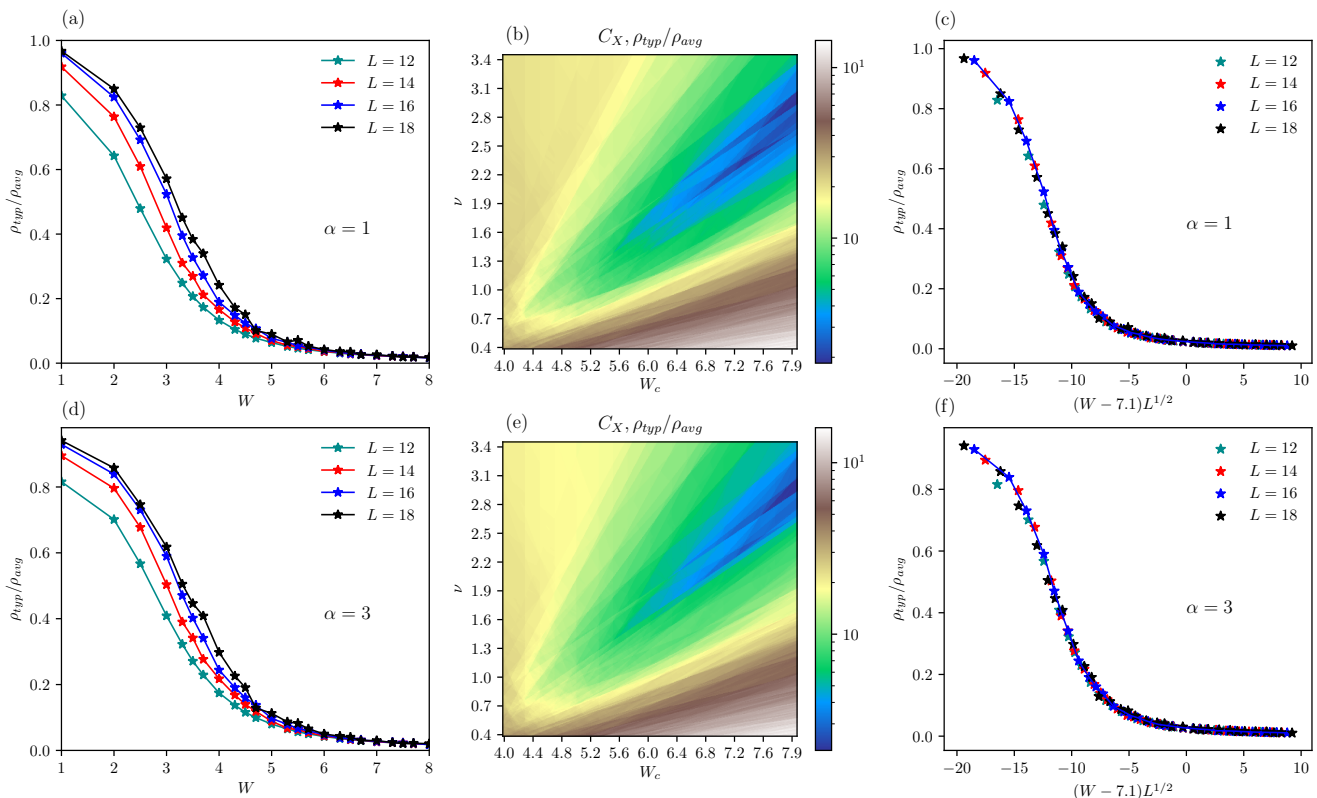


FIG. 1: Panel (a): The ratio of the typical to average local DOS  $\rho_{typ}(\omega = \mu_{eff})/\rho_{avg}(\omega = \mu_{eff})$  for system sizes  $L = 12, 14, 16, 18$  plotted as a function of the disorder strength  $W$  for  $\alpha = 1$ . The ratio is of order one for  $W \ll W_c$  and for  $W > W_c$ , it is vanishingly small. Panel (b): The cost function  $C_X$  (in Eq. 2) as a function of the critical disorder strength  $W_c$  and the correlation length exponent  $\nu$  for  $\alpha = 1$ . Panel (c): The ratio of the typical to average value of local DOS  $\rho_{typ}(\omega = \mu_{eff})/\rho_{avg}(\omega = \mu_{eff})$  plotted as a function of scaled disorder strength  $(W - W_c)L^{1/\nu}$  for  $\alpha = 1$ .  $W_c \approx 7.1$ ,  $\nu \approx 2.5$  correspond to the region of the cost function shown in the middle panel with the minimum value of  $C_x$ . The bottom three panels depict the same quantities for  $\alpha = 3$ . The calculations are done in the middle of the energy band for a rescaled energy bin  $E \in [0.495, 0.505]$ .

ever single-particle Green's functions in real space have attracted attention in the analysis of the MBL phase only recently [59, 60]. We concentrate on the single particle Green's functions in real space in this study, which have been widely utilised to analyse Anderson localization in non-interacting models [61]. We analyse the finite size scaling of the corresponding local density of states (LDOS) and the scattering rates and demonstrate that the ratio of the typical to average value of the local density of states as well as the scattering rates both adhere to the single parameter scaling  $X[L, W] \sim \bar{X}((W - W_c)L^{1/\nu})$  with the critical exponent satisfying the CCFS inequality for a finite value of  $W_c$ . Notably, we observe a good quality scaling collapse with  $\nu \geq 2/d$  for the ratio of the typical to average value of the LDOS as well as the scattering rates not only for the system with nearest neighbour interactions but also for a whole class of one dimensional models with power-law interactions of different ranges and nearest neighbour hopping. The

transition occurs nearly at the same value of the critical disorder  $W_c$  for all ranges of interactions studied. Finite size scaling of eigenlevel spacing ratio, on the other hand, does not satisfy the CCFS bound of the critical exponent which is consistent with earlier studies [5, 20, 46, 47].

We study a class of one-dimensional models of spinless fermions in the presence of random disorder and power-law interactions. The Hamiltonian of the models studied is

$$H = -t \sum_i [c_i^\dagger c_{i+1} + h.c.] + \sum_i \epsilon_i n_i + \sum_{ij} V_{ij} n_i n_j \quad (1)$$

with periodic boundary conditions. Here, the onsite potential  $\epsilon_i \in [-W/t, W/t]$  (uniformly distributed) with  $W$  as the disorder strength. We study power-law interactions with  $V_{ij} = \frac{V}{|r_i - r_j|^\alpha}$ , where  $\alpha$  fixes the range of interactions. We have considered  $\alpha = 1, 2$  and  $3$  in this study. We also consider the limit of the very short range interactions by studying the case of nearest neighbour interactions with  $V_{i,i+1} = V$  and  $V_{ij} = 0$  for  $|j - i| > 1$ .

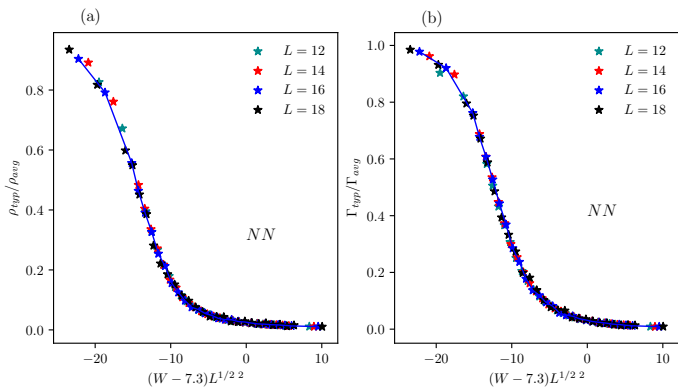


FIG. 2: Left panel: The ratio of the typical to average local DOS  $\rho_{typ}(\omega=0)/\rho_{avg}(\omega=0)$  for different system sizes plotted as a function of the scaled disorder strength  $(W - W_c)L^{1/\nu}$ . The critical disorder  $W_c = 7.3t$  and the exponent  $\nu = 2.2$  are obtained by minimising the cost function  $C_X$  (in Eq. 2) details of which are shown in the SM [74]. A similar trend is seen in the ratio of typical to average value of the scattering rate  $\Gamma_{typ}(\omega=0)/\Gamma_{avg}(\omega=0)$  shown in the right panel. All quantities are computed for system with nearest neighbour interactions and for states in the middle of the eigenspectrum for a rescaled energy bin  $E \in [0.495, 0.505]$

In the entire analysis we fix  $V = t (= 1)$  and the system is half-filled. We study the model using full diagonalization, for the several system sizes from  $L = 12$  to  $L = 18$ . We evaluate the Green's function in the  $n$ th eigenstate  $G_n(i, j, t) = -i\Theta(t)\langle\Psi_n|\{c_i(t), c_j^\dagger(0)\}|\Psi_n\rangle$ , where  $i, j$  are lattice site indices, and the associated self energy  $\Sigma_n(\omega) \equiv \mathbf{G}_0^{-1}(\omega) - \mathbf{G}_n^{-1}(\omega)$  where  $\mathbf{G}_0(\omega)$  is the non-interacting Green's function of the disordered system. The LDOS  $\rho_n(i, \omega)$  and scattering rate are obtained from the imaginary part of the Green's function and the self energy respectively as  $\rho_n(i, \omega) = (-\frac{1}{\pi}) \text{Im}[G_n(i, i, \omega^+)]$  and  $\Gamma_n(i, \omega) = -\text{Im}[\Sigma_n(i, i, \omega)]$ .

The transition from the delocalized to the MBL phase is seen in the disordered averaged Green's function calculated for the mid spectrum eigen-states with rescaled energy  $E_n \sim 0.5$ . The single-particle excitations are exponentially unlikely to be excited in the MBL phase at large scales though the excitations typically propagate up to large scale in the delocalized phase [59]. We analyse the ratio of typical to average value of the LDOS and scattering rates for  $\omega = \mu_{eff}$  where  $\mu_{eff}$  is the effective chemical potential of the system. Here, the typical value is obtained by calculating the geometric average over the lattice sites, energy bin and various independent disorder configurations. The relevant details of our computations are presented in supplemental materials [74].

**Finite-size Scaling Analysis:** We assume that the characteristic length scale diverges with a power law at

the MBL transition point  $\xi \sim |W - W_c|^{-\nu}$ . As a result a normalized observable  $X$  obeys the scaling  $X[\delta, L] \sim \bar{X}(\delta L^{1/\nu})$  with  $\delta = W - W_c$ . To have a quantitative estimate of the scaling collapse, we calculate the cost-function for the quantity  $\{X_i\}$  [53, 62].

$$C_X = \frac{\sum_{j=1}^{N_{total}-1} |X_{j+1} - X_j|}{\max\{X_j\} - \min\{X_j\}} - 1 \quad (2)$$

Here  $N_{total}$  is the total number of values of  $\{X_i\}$  for various values of disorder  $W$  and system sizes  $L$ . We arrange all  $N_{total}$  values of  $\{X_i\}$  according to increasing values of  $(W - W_c)L^{1/\nu}$ .  $C_X$  should be zero close for a perfect data collapse but for the finite size data that we have, we look for a minimum of the cost function with respect to the exponent  $\nu$  for  $W_c$  values which are close to the intuitive guess of the transition point. We study the ratios of typical to average LDOS and scattering rates introduced earlier using a single parameter scaling form ( $X[\delta, L] \sim \bar{X}(\delta L^{1/\nu})$ ), which has also been used to study scaling properties of other quantities relevant in context of MBL [5, 20, 46, 47]. As we will show shortly, this scaling ansatz results in very good scaling collapse for these quantities. Below we first discuss the scaling for the system with power-law interactions followed by the results for the system with nearest neighbour interactions.

Panel (a) of Fig. 1 shows the ratio of the typical to average value of the LDOS for the system with power-law interactions and  $\alpha = 1$ . For weak disorder, the typical value of the LDOS is of the order of the average LDOS while for large values of  $W$  in the MBL phase the typical value of the LDOS becomes vanishingly small though the corresponding average value is still finite. The ratio of typical to average value of LDOS increases with the system size for weak disorder while for very large disorder it becomes essentially independent of the chain size. Interestingly, at the disorder value where the ratio becomes independent of the system size, it also becomes constant with respect to disorder  $W$  within numerical precision and we use this criterion to estimate the transition point. In order to obtain the best scaling collapse of the finite size data for the ratio of typical to average values of the LDOS, we calculated the cost function  $C_X$  which is shown in panel (b) of Fig. 1 for  $\alpha = 1$ .  $C_X$  decreases as the value of the parameter  $W_c$  is increased from  $5t$ , having a broad minima for  $7.1t \leq W_c \leq 7.9t$  and  $2.3 \leq \nu \leq 2.7$ . With further increase in  $W_c$  and  $\nu$ ,  $C_X$  shows a slow increase. Using our estimate of the transition point, explained above, we chose  $W_c = 7.1t$  for which  $C_X$  has a minimum for  $\nu = 2.5$ . The finite size scaling collapse for a fixed value of the critical disorder and the exponent  $\nu$  obtained from minimization of the cost function is shown in panel (c) of Fig. 1. The bottom panel in Fig. 1 shows similar plots for  $\alpha = 3$ . As one can see that the finite size scaling and the minimization of the cost function provides a critical point  $W_c$  which is

very close to the one obtained for  $\alpha = 1$  and again the critical exponent  $\nu \sim 2.5$ . In fact, the critical disorder  $W_c$  and the critical exponent  $\nu$  do not change with the increase in the range of interaction even for  $\alpha = 0.5$ . We also studied the finite size scaling of the ratio of typical to average value of scattering rates and obtain almost the same transition point and critical exponent  $\nu$  as that from the LDOS, details of which are provided in the Supplemental Materials(SM) [74].

Further, we analyse the LDOS and scattering rates for the system with nearest neighbour interactions. Fig. 2 shows the finite size scaling for the ratio of the LDOS and the scattering rates. Again, we observe a very good data collapse for  $W_c = (7.3 \pm 0.3)t$  and  $\nu = 2.2 \pm 0.2$  for both the quantities. The corresponding cost function plots, which are very similar to the one shown for the system with power-law interactions, are shown in the SM [74]. We also analysed the behaviour of the level spacing ratio, which is frequently used to study the MBL transition, and found that the finite size scaling of the level spacing ratio does not satisfy the CCFS bound for the critical exponent in agreement with many earlier works [5, 20, 46, 47]. The cost function in the  $W_c - \nu$  plane has a very different pattern for the level spacing ratio compared to the LDOS and scattering rates studied above. For the level spacing ratio, cost function has a minimum at very small values of  $W_c \sim 5.3t$  and  $\nu = 0.64$ . With further increase in  $W_c$  and  $\nu$  the cost function shows a rapid increase. Details of the cost function and the scaling collapse for the level spacing ratio have been discussed in the SM [74].

**Conclusions and Discussions:** The MBL transition involves many higher excited states and entails a transition from the delocalized phase, where eigenstates are extended and obey volume law of entanglement, to the localised side, where eigenstates are localised and obey area law of entanglement. This makes the MBL transition an atypical transition which does not necessarily follow the standard paradigm for classifying phase transitions. Understanding the nature of the MBL transition is thus central to the problem.

In this work, we present strong evidence in favour of a continuous delocalization to MBL transition where the correlation length exponent obeys the CCFS criterion. This is especially significant in light of recent disagreements and controversies regarding the nature of the MBL transition and the stability of the MBL phase. We show how the ratio of typical to average LDOS and scattering rates can be used to characterise the delocalization to MBL transition. Our analysis also demonstrates that the MBL phase exists in a system with uniform long-range interactions and nearest neighbour hopping, which is consistent with existing theoretical [63–68] and experimental studies [69–71]. The MBL transition even in systems with uniform long-range interactions is continuous in nature.

Although the ratio of typical to average LDOS and the scattering rate scales with a single parameter such that the critical exponent  $\nu \geq 2/d$  with a finite value of the transition point, the level spacing ratio scales with a critical exponent that is much smaller than  $2/d$  and is intriguingly quite close to the one obtained from scaling the local self energy in the Fock space [58] as well as to the correlation length exponent for the Anderson model on random regular graphs [72, 73]. This is consistent with the idea that the effective Anderson model for the MBL system lives in a Fock space that can be compared to a random regular graph with variable connectivity between nodes. Certain physical quantities, such as level spacing ratio and entanglement, appear to follow the critical exponent of the correlation length in the Fock space, whereas others, such as single particle LDOS, appear to adhere to the system’s physical dimension and obey the standard CCFS bound.

Our scaling analysis of single particle LDOS and scattering rates is consistent with the renormalization group calculations, which predicted a continuous MBL transition with the critical exponent  $\nu \geq 2/d$  [32–36]. The search for additional physical quantities that can shed more light on the nature of the MBL transition is unquestionably critical.

A.G. acknowledges Science and Engineering Research Board (SERB) of Department of Science and Technology (DST), India under grant No. CRG/2018/003269 for financial support. A.G. also acknowledges National Supercomputing Mission (NSM) for providing computing resources of ‘PARAM Shakti’ at IIT Kharagpur, which is implemented by C-DAC and supported by the Ministry of Electronics and Information Technology (MeitY) and Department of Science and Technology (DST), Government of India. V.R.C acknowledges funding from the Department of Atomic Energy, India under the project number 12-R&D-NIS-5.00-0100.

- 
- [1] P. W. Anderson, Phys. Rev. **109**, 1492 (1958).
  - [2] D. M. Basko, I. L. Aleiner, and B. L. Altshuler, Ann. Phys. (Amsterdam), **321**, 1126 (2006).
  - [3] E. Altman and R. Vosk, Ann. Rev. Cond. Matt. Phys. **6**, 383 (2015); E. Altman, Nature Physics, **14**, 979 (2018); F. Alet, and N. Laflorencie, C. R.Physique **19**, 498 (2018); R. Nandkishore and D. A. Huse, Ann. Rev. Cond. Mat. Phys. **6**, 15 (2015); D. A. Abanin, E. Altman, I. Bloch, and M. Serbyn, Rev. Mod. Phys. **91**, 021001 (2019).
  - [4] V. Oganesyan and D. A. Huse, Phys. Rev. B **75**, 155111 (2007).
  - [5] D. J. Luitz, N. Laflorencie, F. Alet, Phys. Rev. B **91**, 081103(R) (2015).

- [6] D. J. Luitz, N. Laflorencie, and F. Alet, Phys. Rev. B **93**, 060201(R) (2016).
- [7] M. Schreiber, S. S. Hodgmann, P. Bordia, H. P. Luschen, M. H. Fischer, R. Vosk, E. Altman, U. Schneider, and I. Bloch, Science **349**, 842 (2015).
- [8] P. Bordia, H. P. Luschen, S. S. Hodgman, M. Schreiber, I. Bloch, and U. Schneider, Phys. Rev. Lett. **116**, 140401 (2016).
- [9] H. P. Luschen, P. Bordia, S. Scherg, F. Alet, E. Altman, U. Schneider, I. Bloch, Phys. Rev. Lett. **119**, 260401 (2017).
- [10] D. J. Luitz, and Y. Bar Lev, Ann. Phys. **529**, 1600350 (2017).
- [11] E. V. H. Doggen, F. Schindler, K. S. Tikhonov, A. D. Mirlin, T. Neupert, D. G. Polyakov, I. V. Gornyi, Phys. Rev. B **98**, 174202 (2018).
- [12] E. V. H. Doggen and A. D. Mirlin, Phys. Rev. B **100**, 104203 (2019).
- [13] T. Chanda, P. Sierant, and J. Zakrzewski, Phys. Rev. B **101**, 035148 (2020).
- [14] A. Kshetrimayum, M. Goihl, and J. Eisert, Phys. Rev. B **102**, 235132 (2020).
- [15] Y. Prasad and A. Garg, Phys. Rev. B **103**, 064203 (2021).
- [16] P. Pöpperl, E. V.H. Diggen, J. F. Karcher, A. D. Mirlin, K. S. Tikhonov, Annals of Phys. **435**, 168486 (2021).
- [17] S. Nandy, F. Evers, and S. Bera, Phys. Rev. B **103**, 085105 (2021).
- [18] Y. Prasad and A. Garg, Phys. Rev. B **105**, 214202 (2022).
- [19] S. Iyer, V. Oganesyan, G. Refael, and D. A. Huse, Phys. Rev. B **87**, 134202 (2013).
- [20] J. A. Kjall, H. H. Bardarson, and F. Pollmann, Phys. Rev. Lett. **113**, 107204 (2014).
- [21] S. Bera, H. Schomerus, F. H-Meisner, and J. H. Bardarson, Phys. Rev. Lett. **115**, 046603 (2015).
- [22] P. Naldesi, E. Ercolessi, and T. Roscilde, SciPost Phys. **1**, 010 (2016).
- [23] X. Li, S. Ganeshan, J. H. Pixley, and S. D. Sarma, Phys. Rev. Lett. **115**, 186601 (2015).
- [24] S. Nag and A. Garg, Phys. Rev. B **96**, 060203(R) (2017).
- [25] J. H. Bardarson, F. Pollmann, and J. E. Moore, Phys. Rev. Lett. **109**, 017202 (2012).
- [26] M. Serbyn, Z. Papic, and D. A. Abanin, Phys. Rev. Lett. **110**, 260601 (2013).
- [27] R. Modak and S. Mukerjee, Phys. Rev. Lett. **115**, 230401 (2015).
- [28] M. Serbyn, Z. Papic, and D. A. Abanin, Phys. Rev. Lett. **111**, 127201 (2013).
- [29] M. Serbyn, Z. Papic, and D. A. Abanin, Phys. Rev. Lett. **111**, 127201 (2013).
- [30] V. Ros, M. Muller, and A. Scardicchio, Nuc. Phys. B **891**, 420 (2015).
- [31] J. Z. Imbrie, Phys. Rev. Lett. **117**, 027201 (2016); J. Z. Imbrie, Journal of Statistical Physics **163**, 998 (2016).
- [32] R. Vosk, D. A. Huse, and E. Altman, Phys. Rev. X **5**, 031032 (2015).
- [33] A. C. Potter, R. Vasseur, and S. A. Parameswaran, Phys. Rev. X **5**, 031033 (2015).
- [34] L. Zhang, B. Zhao, T. Devakul, and D. A. Huse, Phys. Rev. B **93**, 224201 (2016).
- [35] P. T. Dumitrescu, R. Vasseur, and A. C. Potter, Phys. Rev. Lett. **119**, 110604 (2017).
- [36] Shi-Xin Zhang and H. Yao, Phys. Rev. Lett. **121**, 206601 (2018).
- [37] J. T. Chayes, L. Chayes, D. S. Fisher, and T. Spencer, Phys. Rev. Lett. **57**, 2999 (1986); J. T. Chayes, L. Chayes, D. S. Fisher, and T. Spencer, Commun. Math. Phys. **120**, 501-523 (1989).
- [38] A. Chandran, C. R. Laumann, and V. Oganesyan, arXiv:1509.04285.
- [39] A. B. Harris, J. Phys. C **7**, 1671 (1974).
- [40] B.I. Shklovskii, B. Shapiro, B.R. Sears, P. Lambrianides, and H. B. Shore, Phys. Rev. B **47**, 11487 (1993).
- [41] I. Kh. Zharekeshev and Bernhard Kramer, Phys. Rev. Lett. **79**, 717 (1997).
- [42] K. Slevin and T. Ohtsuki, Phys. Rev. Lett. **82**, 382 (1999).
- [43] E. Tarquini, G. Biroli, and M. Tarzia, Phys. Rev. B **95**, 094204 (2017).
- [44] T. Devakul and D. A. Huse, Phys. Rev. B **96**, 214201 (2017).
- [45] P. Sierant, M. Lewenstein, A. Scardicchio, and J. Zakrzewski, arXiv:2203.15697.
- [46] V. Khemani, D. N. Sheng, and D. A. Huse, Phys. Rev. Lett. **119**, 075702 (2017).
- [47] P. Sierant and J. Zakrzewski, Phys. Rev. B **99**, 104205 (2019).
- [48] A. Goremykina, R. Vasseur, and M. Serbyn, Phys. Rev. Lett. **122**, 040601 (2019).
- [49] P. T. Dumitrescu, A. Goremykina, S. A. Parameswaran, M. Serbyn, and R. Vasseur, Phys. Rev. B **99**, 094205 (2019).
- [50] A. Morningstar and D. A. Huse, Phys. Rev. B **99**, 224205 (2019).
- [51] D. J. Luitz, F. m. c. Huveneers, and W. De Roeck, Phys. Rev. Lett. **119**, 150602 (2017).
- [52] A. Morningstar, D. A. Huse, and J. Z. Imbrie, Phys. Rev. B **102**, 125134 (2020).
- [53] J. Šuntajs, J. Bonca, T. Prosen, and L. Vidmar, Phys. Rev. B **102**, 064207 (2020).
- [54] N. Laflorencie, G. Lemarié, and N. Macé, Phys. Rev. Research **2**, 042033 (2020).
- [55] M. Hopjan, G. Orso, and F. Heidrich-Meisner, Phys. Rev. B **104**, 235112 (2021).
- [56] D. E. Logan and S. Welsh, Phys. Rev. B **99**, 045131 (2019).
- [57] S. Roy and D. E. Logan, Phys. Rev. B **101**, 134202 (2020).
- [58] J. Sutradhar, S. Ghosh, S. Roy, D. E. Logan, S. Mukerjee, and S. Banerjee, Phys. Rev. B **106**, 054203 (2022).
- [59] A. Jana, V. R. Chandra, and A. Garg, Phys. Rev. B **104**, L140201 (2021).
- [60] N. Roy, J. Sutradhar, S. Banerjee, arXiv:2208.10714.
- [61] *50 years of Anderson localization*, by E. Abrahams, World Scientific Publishing (2010).
- [62] S. M. Bhattacharjee and F. Seno, J. Phys. A: Math. Gen. **34**, 6375 (2001).
- [63] A. L. Burin, arXiv:cond-mat/0611387; A. L. Burin, Phys. Rev. B **91**, 094202 (2015).
- [64] N. Y. Yao, C. R. Laumann, S. Gopalakrishnan, M. Knap, M. Muller, E. A. Demler, and M. D. Lukin, Phys. Rev. Lett. **113**, 243002 (2014).
- [65] D. B. Gutman, I. V. Protopopov, A. L. Burin, I. V. Gornyi, R. A. Santos, and A. D. Mirlin, Phys. Rev. B **93**, 245427 (2016).
- [66] K. S. Tikhonov and A. D. Mirlin, Phys. Rev. B **97**, 214205 (2018).
- [67] S. Nag and A. Garg, Phys. Rev. B **99**, 224203 (2019).

- [68] S. Roy and D. E. Logan, *SciPost Phys.* **7**, 042 (2019).
- [69] J. Zhang, P. Hess, A. Kyprianidis, P. Becker, A. Lee, J. Smith, G. Pagano, I. D. Potirniche, A. C. Potter, A. Vishwanath et al., *Nature* **543**, 217 (2017).
- [70] S. Choi, J. Choi, R. Landig, G. Kucsko, H. Zhou, J. Isoya, F. Jelezko, S. Onoda, H. Sumiya, V. Khemani et al., *Nature* **543**, 221 (2017).
- [71] J. Smith, A. Lee, P. Richerme, B. Neyenhuis, P. W. Hess, P. Hauke, M. Heyl, D. A. Huse, and C. Monroe, *Nat. Phys.* **12**, 907 (2016).
- [72] M. Pino, *Phys. Rev. Res.* **2**, 042031 (R) (2020).
- [73] V. Kravtsov, B. Altshuler, and L. Ioffe, *Ann. Phys.* **389**, 148 (2018).
- [74] See supplementary material.
- [75] V. V. Volchkov, M. Pasek, V. Denechaud, M. Mukhtar, A. Aspect, D. Delande, and V. Josse, *Phys. Rev. Lett.* **120**, 060404 (2018).

**Supplementary material for “Universal Properties of single particle excitations across the many-body localization transition”**

Atanu Jana<sup>1,3</sup>, V. Ravi Chandra<sup>1,3</sup>, Arti Garg<sup>2,3</sup>

<sup>1</sup> *School of Physical Sciences, National Institute of Science Education and Research Bhubaneswar, Jatni, Odisha 752050, India*

<sup>2</sup> *Theory Division, Saha Institute of Nuclear Physics,  
1/AF Bidhannagar, Kolkata 700 064, India and*

<sup>3</sup> *Homi Bhabha National Institute, Training School Complex, Anushaktinagar, Mumbai 400094, India*

## DETAILS OF CALCULATIONS AND DISORDER AVERAGING

We compute the disorder averaged LDOS and scattering rates for  $\alpha = 1, 2, 3$  and the nearest neighbour cases of the Hamiltonian in Eq.(1) of the main text. The LDOS and scattering rates are extracted from the Lehmann representation of the Green's function  $G_n(i, j, \omega)$  whose diagonal element is given by:

$$G_n(i, i, \omega^+) = \sum_m \frac{|\langle \Psi_m | c_i^\dagger | \Psi_n \rangle|^2}{\omega + i\eta - E_m + E_n} + \frac{|\langle \Psi_m | c_i | \Psi_n \rangle|^2}{\omega + i\eta + E_m - E_n} \quad (1)$$

We calculate the LDOS and the scattering rates for the many-body eigenstates in the middle of the spectrum, that is with a rescaled energy bin  $E \in [0.495, 0.505]$  for a large number of independent disorder realisations. For each value of  $\alpha$  we use 15000, 1000, 500 and 50 realisations of disorder for  $L = 12, 14, 16, 18$  respectively to calculate the averages of the LDOS and scattering rates. The value of  $\omega$  for each  $\alpha$  is chosen to be  $\omega = \mu_{eff} = \sum_{|j-i|=1}^{L/2} \frac{1}{|j-i|^\alpha}$  (for  $V = 1$ ) which is the effective chemical potential of the system under the assumption that the disorder averaged system will respect particle hole symmetry. The infinitesimal  $\eta$  is chosen to be  $10^{-2}$ . For the system with nearest neighbour interactions we have shown results for  $\omega = 0$ . The LDOS  $\rho_{typ}(\omega)$  and the scattering rate  $\Gamma_{typ}(\omega)$  are very flat around  $\omega = 0$  over a width of around  $2W$  and  $\mu_{eff}$  for nearest neighbour interaction is  $V/2$ . Thus, effectively the behaviour of LDOS and scattering rate at  $\omega = \mu_{eff}$  and  $\omega = 0$  is the same for the system with nearest neighbour interactions. For the system with nearest neighbour interactions, we use 15000, 10000, 3000, 200 realization of disorder for  $L = 12, 14, 16, 18$  respectively to calculate the averages of level spacing ratio. For the disorder averaging of the LDOS and scattering rates, we used 15000, 1000, 500 configurations of disorder for  $L = 12, 14, 16$  and 50 – 100 configurations for  $L = 18$ .

## FINITE-SIZE SCALING OF SINGLE PARTICLE SCATTERING RATES

In the main text in Fig. 1 we analyzed the finite-size scaling of single particle LDOS for the system with power-law interactions. We now present details of the finite size scaling for the scattering rates. In Fig. 1, in the top row we present the data for the system with  $\alpha = 1$ . In the top left panel we show the ratio of typical to average value of the scattering rate  $\Gamma_{typ}(\omega)/\Gamma_{avg}(\omega)$  obtained from the middle of the many-body eigenspectrum and  $\omega = \mu_{eff}$ . In sharp similarity to the LDOS, the ratio of typical to average value of the scattering rate is of order one for weak disorder and becomes vanishingly small and size independent for very large values of disorder. In order to determine the nature of the transition, we did the finite size scaling. As mentioned in the main paper, we calculated the cost function  $C_X$  to quantify the finite size scaling collapse. In the top middle panel we show the color plot of the cost function in  $W_c - \nu$  plane.  $C_X$  is very large for small values of  $W_c$  for any value of  $\nu$  considered. For slightly larger values of  $W_c$ ,  $C_X$  has a non-monotonic dependence on  $\nu$  such that  $C_X$  first decrease as  $\nu$  increases, attains a minima and then starts increasing again. The best minima obtained in the range of parameters considered, occurs for  $7.1 \leq W_c \leq 7.9$ . We opt the minimum value of  $W_c = 7.1t$  for which  $C_X$  shows a minimum for  $2.3 \leq \nu \leq 2.7$ . The rightmost panel in the top row shows the scaling collapse as a function of the scaled disorder  $(W - W_c)L^{1/\nu}$  with  $W_c = 7.1t$  and  $\nu = 2.5$ . We would like to emphasize that the ratio of typical to average scattering rate obeys the single parameter scaling and show a good quality data collapse for the value of the exponent  $\nu \geq 2$  which satisfies the CCFS inequality. In the lower row of Fig. 1 we have shown similar plots for  $\alpha = 3$  which correspond to a shorter range of interactions. As shown here the critical point  $W_c$  and the critical exponent  $\nu$  are almost independent of the range of interactions.

## COST FUNCTIONS FOR THE SYSTEM WITH NEAREST NEIGHBOUR INTERACTIONS

In the main text in Fig. 2 we have shown the scaling collapse for the LDOS and scattering rate for the system with nearest neighbour interactions. Here, we provide the supporting calculation of the cost function which was minimised to obtain the critical point and the critical exponent used in the scaling collapse plot. It is interesting to notice that not only the qualitative features of the cost function but also the region of minima in  $W_c - \nu$  plane is almost the same for all the range of interaction considered.

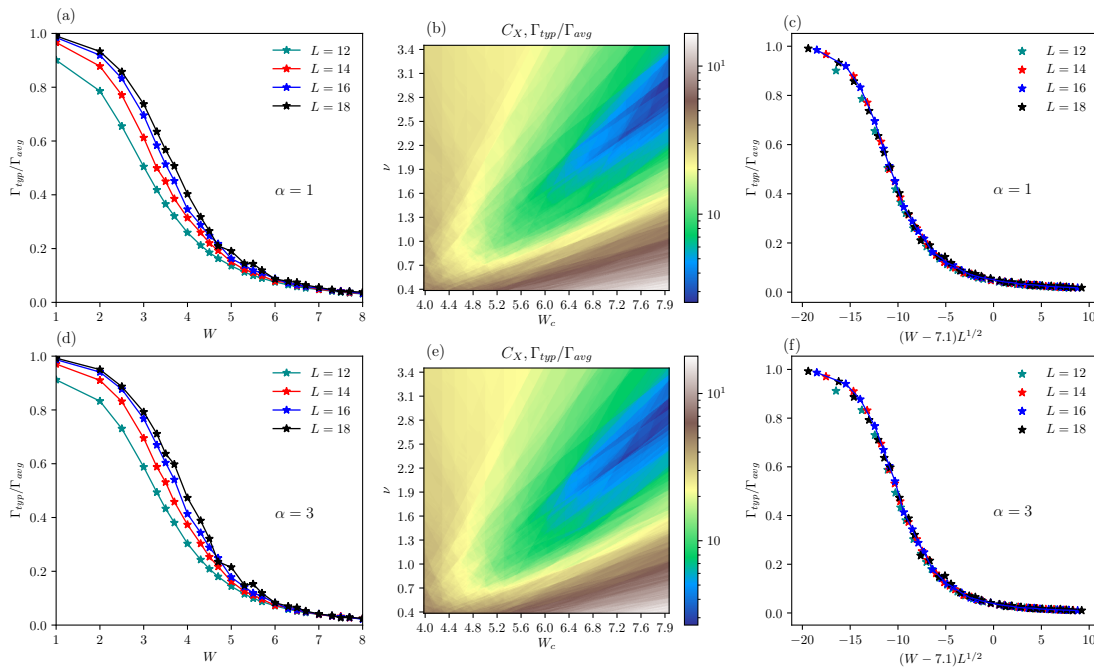


FIG. 1: Panel(a) shows the ratio of the typical to average values of scattering rate  $\Gamma_{typ}(\omega)/\Gamma_{avg}(\omega)$  at  $\omega = \mu_{eff}$ , as a function of disorder  $W$  for various system sizes and  $\alpha = 1$ . Panel(b) shows the cost function  $C_X$  calculated for  $X = \Gamma_{typ}(\omega = \mu_{eff})/\Gamma_{avg}(\omega = \mu_{eff})$  in  $W_c - \nu$  plane. The cost function has a broad minimum for  $7.1 \leq W_c \leq 7.9$ .  $W_c = 7.1$  corresponds to the minimum of the cost function for  $2.3 \leq \nu \leq 2.7$ . Panel (c) shows the scaling collapse for  $\Gamma_{typ}(\omega = \mu_{eff})/\Gamma_{avg}(\omega = \mu_{eff})$  as a function of the scaled disorder  $(W - W_c)L^{1/\nu}$  for  $W_c = 7.1t$  and  $\nu = 2.5$ . Similar trend of the scattering rates, the corresponding cost function and the scaling collapse is seen for  $\alpha = 3$  in the bottom row panels. Scattering rate  $\Gamma(\omega)$  has been computed for states in the middle of the eigenspectrum for a rescaled energy bin  $E \in [0.495, 0.505]$ .

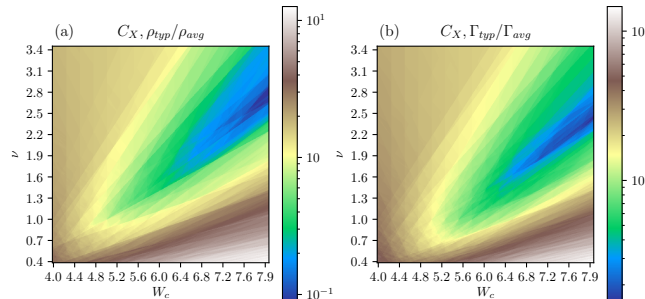


FIG. 2: The left panel shows the cost function  $C_X$  in the  $W_c - \nu$  plane for  $X = \rho_{typ}(\omega = 0)/\rho_{avg}(\omega = 0)$  and the right panel shows  $C_X$  for  $X = \Gamma_{typ}(\omega = 0)/\Gamma_{avg}(\omega = 0)$ . In the right panel, the cost function has minimum around  $W_c = 7.3$  for  $2.0 \leq \nu \leq 2.4$ . In the left panel, a broad minimum of  $C_X$  exists for  $7.1 \leq W_c \leq 7.9$  and  $\nu = 2.4 \pm 0.3$ .

### FINITE SIZE SCALING FOR LEVEL SPACING RATIO

In this section we compare the behaviour of a commonly used diagnostic of the transition, namely the level spacing ratio with the disorder averaged local density of states and the scattering rates obtained from the Green's functions. The level spacing ratios  $r_n$  are defined in the usual way  $r_n = \frac{\min(\delta_n, \delta_{n+1})}{\max(\delta_n, \delta_{n+1})}$ , where,  $\delta_n = E_{n+1} - E_n$ . Fig. 3 shows the plot of disorder averaged  $r_n$  vs disorder  $W$  for various system sizes for the system with nearest neighbour interactions. Level spacing ratio obeys Wigner-Dyson statistics for weak disorder and in the very strong disorder limit it obeys

the Poissonian statistics. To determine the nature of transition in the level spacing ratio as the disorder strength is increased, we did the finite size scaling assuming the single parameter ansatz mentioned in the main text. The cost function  $C_X$  for the level spacing ratio is shown in the middle panel of Fig. 3 which has a very different trend in  $W_c - \nu$  plane as compared to the cost function for the LDOS and scattering rates.  $C_x$  for the level spacing ratio has a minima for  $\nu = 0.64$  and it increases as  $\nu$  increases beyond 0.64.

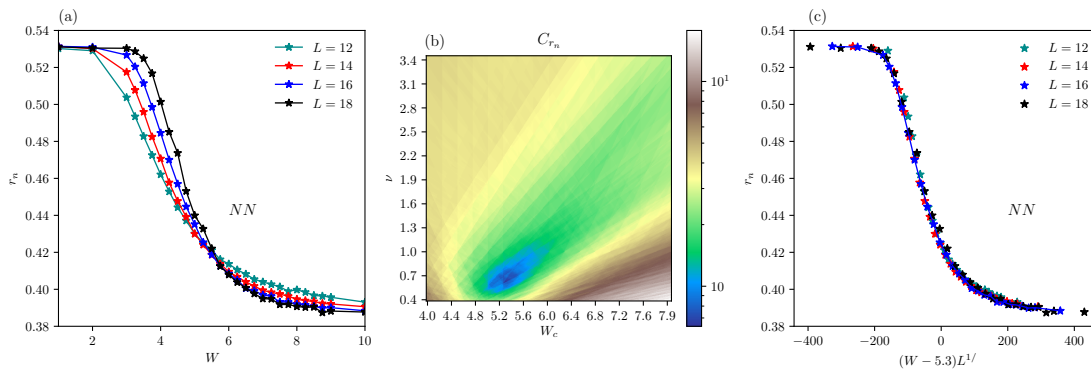


FIG. 3: Panel(a) shows the level spacing ratio as a function of disorder  $W$  for various system sizes for the system with nearest neighbour interactions. Here  $r_n$  has been calculated for middle of the many-body eigenspectrum for a rescaled energy bin  $E \in [0.495, 0.505]$ . The cost function  $C_X$  for the level spacing ratio has been shown in panel (b). The cost function has a minimum for  $W_c \sim 5.3 \pm 0.1$  and  $\nu = 0.6 \pm 0.1$ . In panel (c) we have shown the scaling collapse using  $W_c = 5.3t$  and  $\nu = 0.64$ .